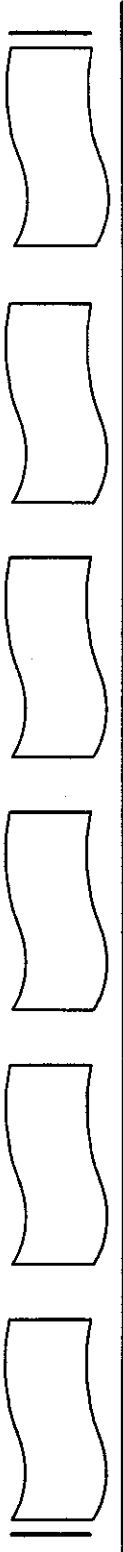


**FED-Vol. 102**

**PVP-Vol. 204**



# **FORUM ON UNSTEADY FLOW — 1990 —**

*presented at*

THE WINTER ANNUAL MEETING OF  
THE AMERICAN SOCIETY OF MECHANICAL ENGINEERS  
DALLAS, TEXAS  
NOVEMBER 25–30, 1990

*sponsored by*

THE FLUIDS ENGINEERING DIVISION AND  
THE PRESSURE VESSELS AND PIPING DIVISION, ASME

*edited by*

PAUL H. ROTHE  
CREARE, INC.

# ROCKET PROPELLANT LINE WATERHAMMER TRANSIENTS IN A VARIABLE-G ENVIRONMENT

T. W. Walters  
Thermodynamics Group  
General Dynamics Space Systems Division  
San Diego, California

## INTRODUCTION

Waterhammer pressure transients are generated in liquid-filled pipes when the velocity of the liquid is increased or decreased. Rapid velocity changes (such as an instantaneous valve closure) can lead to very high pipe pressures that may damage the piping system. The fundamental equations of waterhammer can be found in standard references (1, 2, 3), and their solution by the method of characteristics has become a straightforward process when performed on a digital computer. To simplify the solution, the equations are generally written in terms of piezometric head, which assumes a constant acceleration due to gravity. An application of the equations to waterhammer occurring in a rocket propellant line required that the equations be formulated so as to include varying system acceleration levels. This formulation was incorporated into a computer program, and comparisons with flight data show good agreement.

## BACKGROUND

Waterhammer in a variable acceleration environment can occur in any fluid system that is not stationary. Because the fluid system is often the method of propulsion in a moving vehicle, rapid changes in vehicle acceleration often occur simultaneously with rapid fluid velocity changes in the vehicle propulsion system. Systems where this may occur include automobiles, aircraft, missiles, and launch vehicles. What is meant by a "variable-g environment" is an acceleration experienced equally by the entire system that varies in magnitude but not direction. This is generally the case for launch vehicles, but may not be the case for the other vehicle systems just mentioned. The modeling of systems where the system acceleration vector varies with direction is beyond the scope of this paper.

## APPLICATION FOR VARIABLE-G WATERHAMMER

Waterhammer pressure transients were investigated in an Atlas/Centaur expendable launch vehicle liquid oxygen ( $\text{LO}_2$ ) propellant line during in-flight booster engine cutoff (BECO). The Atlas II, a new version of Atlas/Centaur currently in development, required a propellant line waterhammer analysis at BECO. For an Atlas II, BECO occurs about 170 seconds after liftoff. Figure 1 depicts an Atlas II vehicle and its

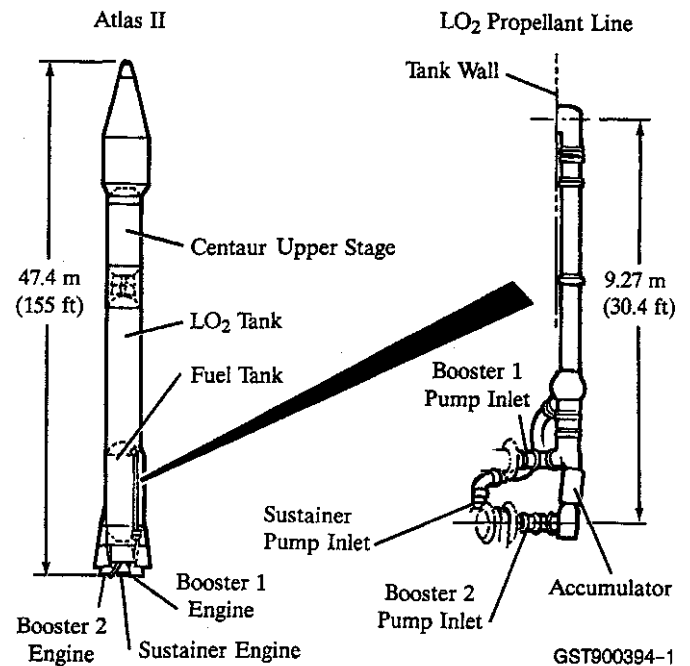


Fig. 1 Atlas II expendable launch vehicle and  $\text{LO}_2$  propellant line

$\text{LO}_2$  line, which feeds three engines. During BECO the two booster engines (B1 and B2) are shut down while the sustainer engine continues to burn, resulting in a rapid system acceleration decay from 5.5 to 0.85 g's due to the reduction in thrust. This g decay and the flowrate decay of the booster engines are shown in Figure 2. The waterhammer pressure transients generated in the  $\text{LO}_2$  line due to engine shutdown occur in this rapidly changing acceleration field.

Initial analyses conservatively assumed a constant 5.5 g's at BECO, but the magnitude of the predicted pressure transients exceeded the 1.32 MPa (192 psi) allowable in the line. An analytical technique was therefore developed to model the variable-g environment, which resulted in acceptable line pressure predictions. Figure 3 shows the predicted pressures at the B2 engine inlet when assuming a constant 5.5 g's, and also

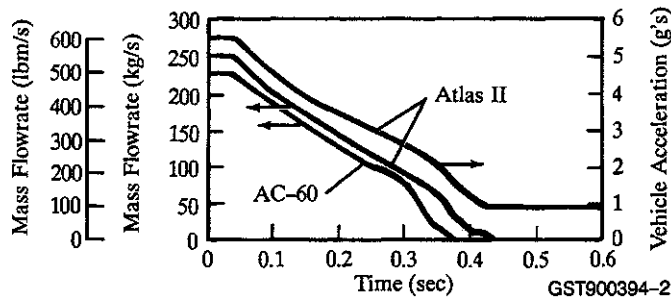


Fig. 2 Atlas booster engine flowrate decay and g decay at BECO

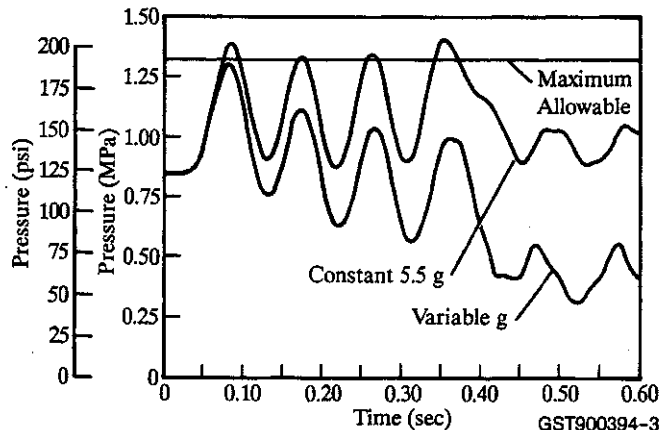


Fig. 3 Predicted waterhammer pressures for Atlas II at B2 engine inlet with and without constant g assumption

shows the pressures when the variable-g curve shown in Figure 2 is modeled. It can be seen that the variable-g model prediction is below the LO<sub>2</sub> line pressure allowable, while the constant 5.5 g model exceeds it. This variable-g approach helped avoid a costly redesign of the LO<sub>2</sub> line.

#### VARIABLE-G ANALYTICAL TECHNIQUE

The fundamental equations of waterhammer for a relatively stiff liquid-filled pipe are (1):

$$gH_x + V_t + \frac{f}{2D} |V| |V| = 0 \quad (1)$$

$$H_t + \frac{a^2}{g} V_x = 0 \quad (2)$$

where Eqn. (1) is the one-dimensional momentum equation, Eqn. (2) is the continuity equation, and the subscripts refer to differentiation with respect to space and time. These two partial differential equations can be solved by the method of characteristics yielding four ordinary differential equations that are solved by finite differences. By integrating the four equations and substituting flowrate,  $Q$ , for velocity,  $V$ , the following difference equations are obtained (1):

$$H_{P_i} = CP - BQ_{P_i} \quad (3)$$

$$H_{P_i} = CM + BQ_{P_i} \quad (4)$$

with the restriction that  $\Delta x/\Delta t = \pm a$ . This approach to differencing the equations is known as the method of specified time intervals.  $CP$  and  $CM$  are constants determined from the solution at the previous time step

$$CP = H_{i-1} + BQ_{i-1} - RQ_{i-1} |Q_{i-1}| \quad (5)$$

$$CM = H_{i+1} - BQ_{i+1} + RQ_{i+1} |Q_{i+1}| \quad (6)$$

The subscript  $P$  refers to the current time step, the subscript  $i$  refers to the position in space, and  $B = a/(gA)$  while  $R = f\Delta x/(2gDA^2)$ . The only unknowns in Eqns. (3-6) are  $H_{P_i}$  and  $Q_{P_i}$ . With the incorporation of boundary conditions to describe the pipe endpoints, the solution can be obtained by marching in time.

Although it is most common to see these equations in terms of piezometric head and flowrate, they can also be written in terms of pressure and flowrate (or velocity). The accurate form of the equations when written in either head or pressure is discussed in (4). The piezometric head is related to pressure

$$H = P/(\rho g_v) + z \quad (7)$$

Inspection of Eqn. (7) shows why it is not possible to solve Eqns. (3) and (4) for nonhorizontal systems when the acceleration is varying. The reason is that the varying vehicle acceleration,  $g_v$ , affects the pressure head but not the elevation head. For systems with elevation differences, Eqns. (3) and (4) must be written with the pressure head and elevation head separated

$$P_{P_i} = \rho g_v (CP - BQ_{P_i} - z_i) \quad (8)$$

$$P_{P_i} = \rho g_v (CM + BQ_{P_i} - z_i) \quad (9)$$

Eqns. (5) and (6) are similarly rewritten to incorporate Eqn. (7)

$$CP = P_{i-1}/(\rho g_v) + z_i + BQ_{i-1} - RQ_{i-1} |Q_{i-1}| \quad (10)$$

$$CM = P_{i+1}/(\rho g_v) + z_i - BQ_{i+1} + RQ_{i+1} |Q_{i+1}| \quad (11)$$

$B$  and  $R$  now vary with time as the system acceleration varies. These equations were incorporated into a computer program, with the acceleration as an input to the program as a function of time.

#### COMPARISON OF VARIABLE-G MODEL TO FLIGHT DATA

Transient waterhammer pressures are not generally measured on Atlas/Centaur vehicles. However, a waterhammer concern on an earlier version of Atlas led to installation of special instrumentation at the B1 and B2 engine turbopump inlets on AC-60, which lifted an Intelsat V into orbit on Sept. 28, 1982 from Cape Canaveral. Since the AC-60 version of Atlas, the vehicle has been lengthened and the booster engine thrust uprated to arrive at the Atlas II (Figure 1). The AC-60 LO<sub>2</sub> line was shorter than Atlas II by 1.81 m (5.94 ft), and the engine flowrates were about 10% lower (Figure 2). In addition, AC-60 did not have an accumulator in the LO<sub>2</sub> line. The AC-60 g decay was qualitatively similar to Atlas II (Figure 2), although the decay occurs about 40 ms faster because of the faster engine shutdown.

The measured pressure for AC-60 is compared to the predicted pressure at the B1 engine inlet in Figure 4 and the B2 engine inlet in Figure 5. Overall good agreement is evident. The first predicted pressure peak in Figures 4 and 5 agrees well with the data, while the following series of predicted peaks are not as pronounced in the data. This may be due to the manner in which the engine flow decay was modeled. The boundary condition for the two booster engines was modeled as a specified flowrate (Figure 2) with pressure waves being totally reflected at the engine boundaries. However, the real system is more complicated, with pressure transients able to transmit through the engine turbopumps to some degree, rather than being totally reflected as in the model.

Another possible explanation is that microbubbles at the turbopump inlets soften the pressure waves. Microbubbles have been observed in the past during flow visualization ground tests. The bubbles form a cloud around the turbopump inducers, which add swirl to the LO<sub>2</sub> just before entering the pumps. Once the pumps slowed sufficiently,

one would expect the microbubbles to disappear because the slower rotation rate of the pump inducers would not cause as severe a disturbance to the flow. This may explain the much larger measured pressure transient after 0.25 second.

It is evident that the predicted pressure peak at 0.33 second in Figures 4 and 5 was not supported by the data. This may be due to the difficulty in predicting the engine flowrate decay in this region by the engine manufacturer. Although the slope of the AC-60 flowrate decay shown in Figure 2 steepens at 0.3 second, the real change in slope at this point may not be quite as severe.

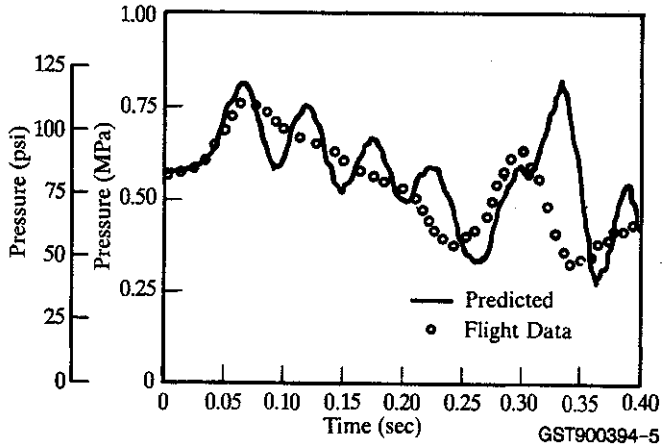


Fig. 4 Predicted pressure vs measured pressure at B1 engine inlet for AC-60

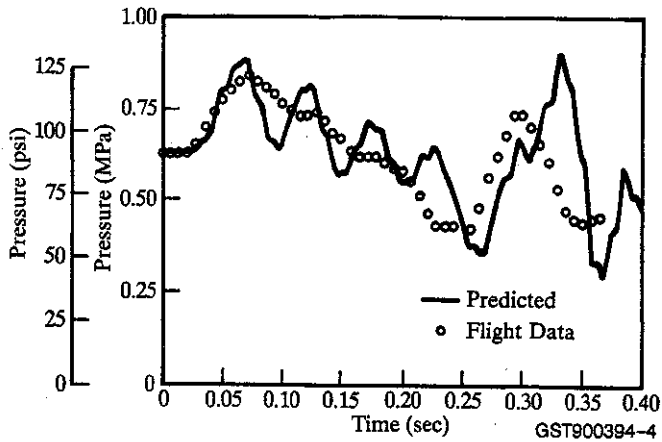


Fig. 5 Predicted pressure vs measured pressure at B2 engine inlet for AC-60

## CONCLUSION

A method for modeling waterhammer transients with the method of characteristics in systems with variable-g environments is described. Comparison of predictions with this technique to flight data for a rocket propellant line show good agreement. The general use of this technique for modeling systems with variable-g environments can remove unnecessary conservatism in predictions.

## NOMENCLATURE

- A = pipe cross-sectional area
- a = wavespeed
- B = pipe impedance,  $a/(gA)$
- D = pipe diameter
- f = Darcy-Weisbach friction factor
- g = acceleration due to gravity
- H = piezometric head
- P = pressure
- Q = volumetric flowrate
- R = pipe resistance,  $f\Delta x/(2gDA^2)$
- t = time
- V = velocity
- x = distance
- z = elevation
- $\rho$  = density

### Subscripts

- i = position
- P = current time step
- t = differentiation with respect to time
- v = vehicle acceleration
- x = differentiation with respect to space

## REFERENCES

1. Wylie, E. B., and Streeter, V. L., *Fluid Transients*, corrected ed., FEB Press, Ann Arbor, MI, 1983.
2. Streeter, V. L., and Wylie, E. B., *Hydraulic Transients*, McGraw-Hill Book Co., New York, NY, 1967.
3. Watters, G. Z., *Modern Analysis and Control of Unsteady Flow in Pipelines*, Ann Arbor Science, Ann Arbor, MI, 1979.
4. Wylie, E. B., "Fundamental Equations of Waterhammer," *Journal of Hydraulic Engineering*, Vol. 110, No. 4, April 1984, pp. 539-542.